Electronic Supplementary Material (ESI) for Journal of Materials Chemistry A.

Supporting Information

High sulfur content microporous carbon coated sulfur composite synthesized via in-situ oxidation of metal sulfide for high-performance Li/S battery

Qian Wang, Zhen-Bo Wang, Chao Li, Da-Ming Gu*

School of Chemistry and Chemical Engineering, Harbin Institute of Technology, No. 92 West-Da Zhi Street, Harbin, 150001 China

*Corresponding author, E-mail: wangzhb@hit.edu.cn (Z.B. Wang)

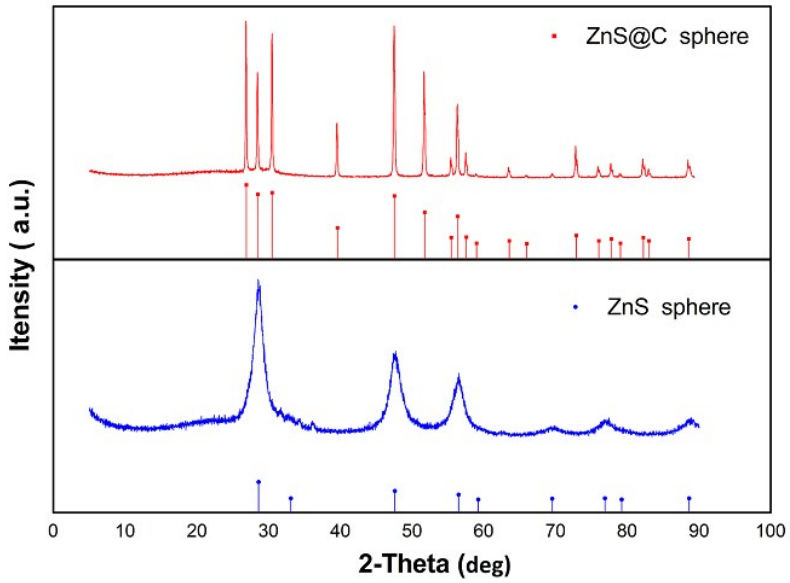

Figure S1. X-ray diffraction patterns of ZnS and ZnS@MPC-2

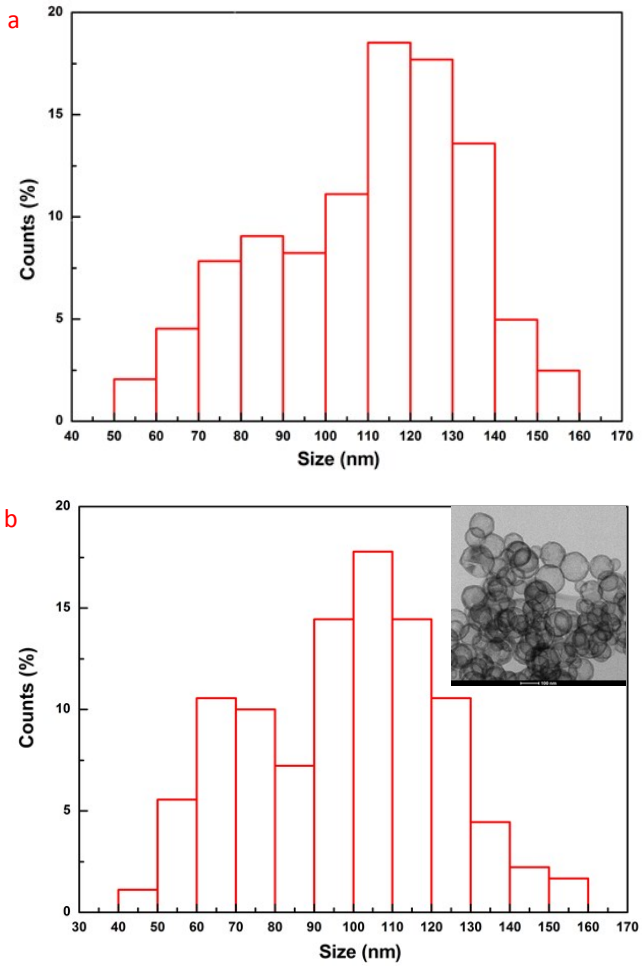

Figure S2. (a) Particle size distribution histograms of ZnS. (b) inner pore diameter size distribution of MPC-HS. The inset shows the TEM of MPC-HS. Scale bar, 100 nm.

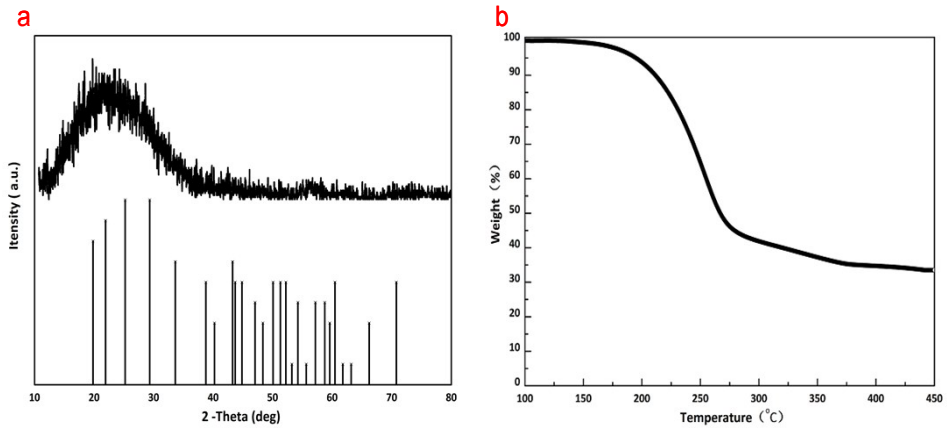

Figure S3. (a) X-ray diffraction pattern, (b) thermal gravimetric analysis of S@MPC-DHS-2

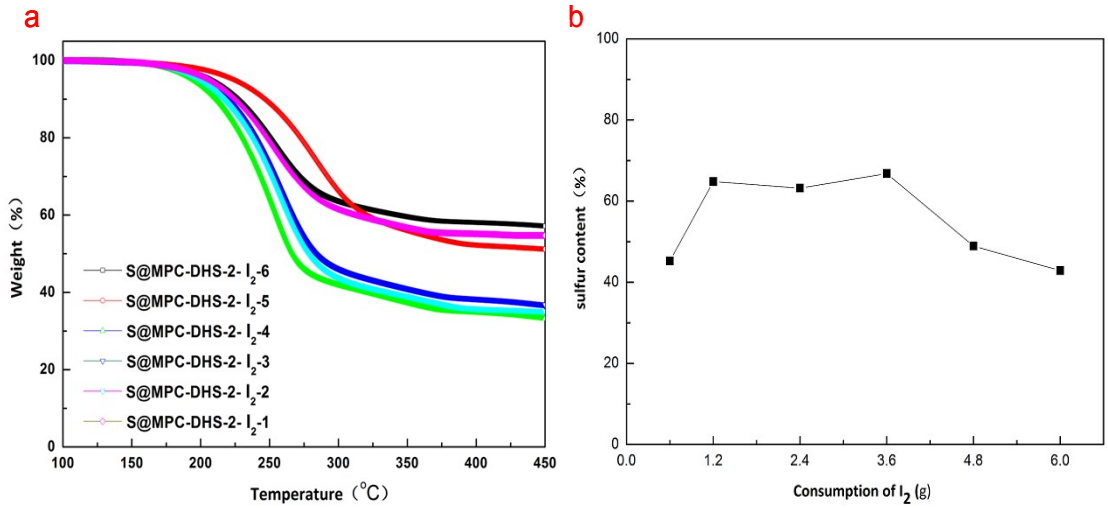

Figure S4. (a)The thermal gravimetric analysis of the S@MPC-DHS-I_2, (b) The sulfur content of S@MPC-DHS-I_2 corresponding to the consumption of I_2 in preparation process.

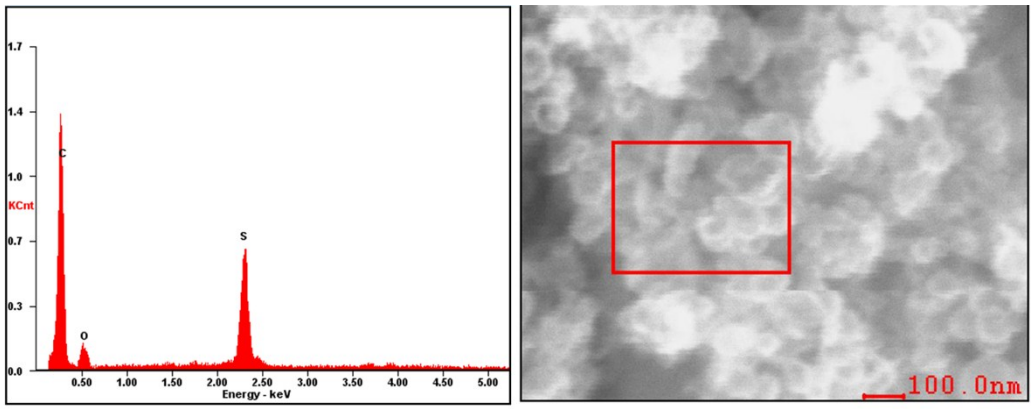

Figure S5. The EDX data of S@MPC-DHS-2.

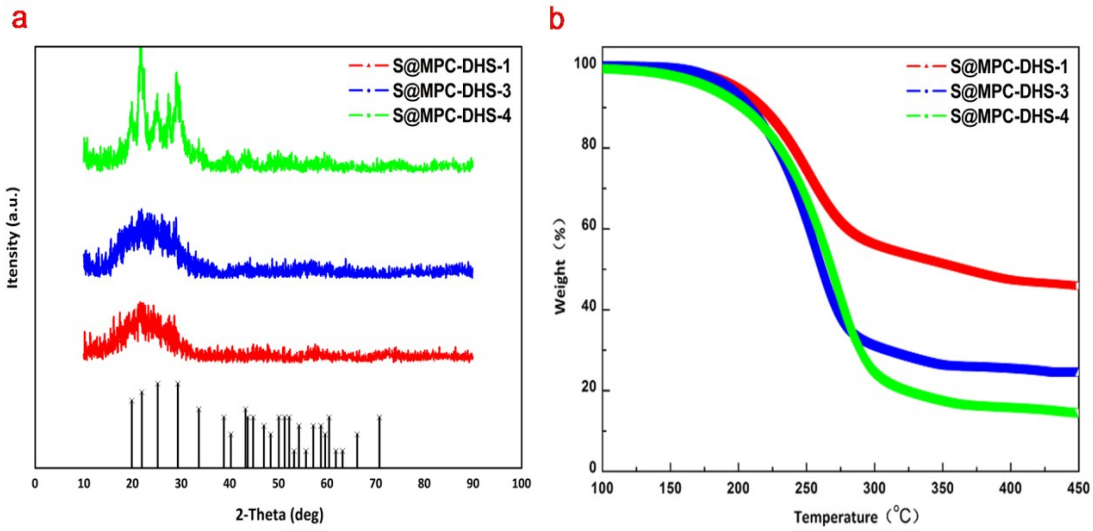

Figure S6. (a)X-ray diffraction pattern, (b) thermal gravimetric analysis of S@MPC-DHS.

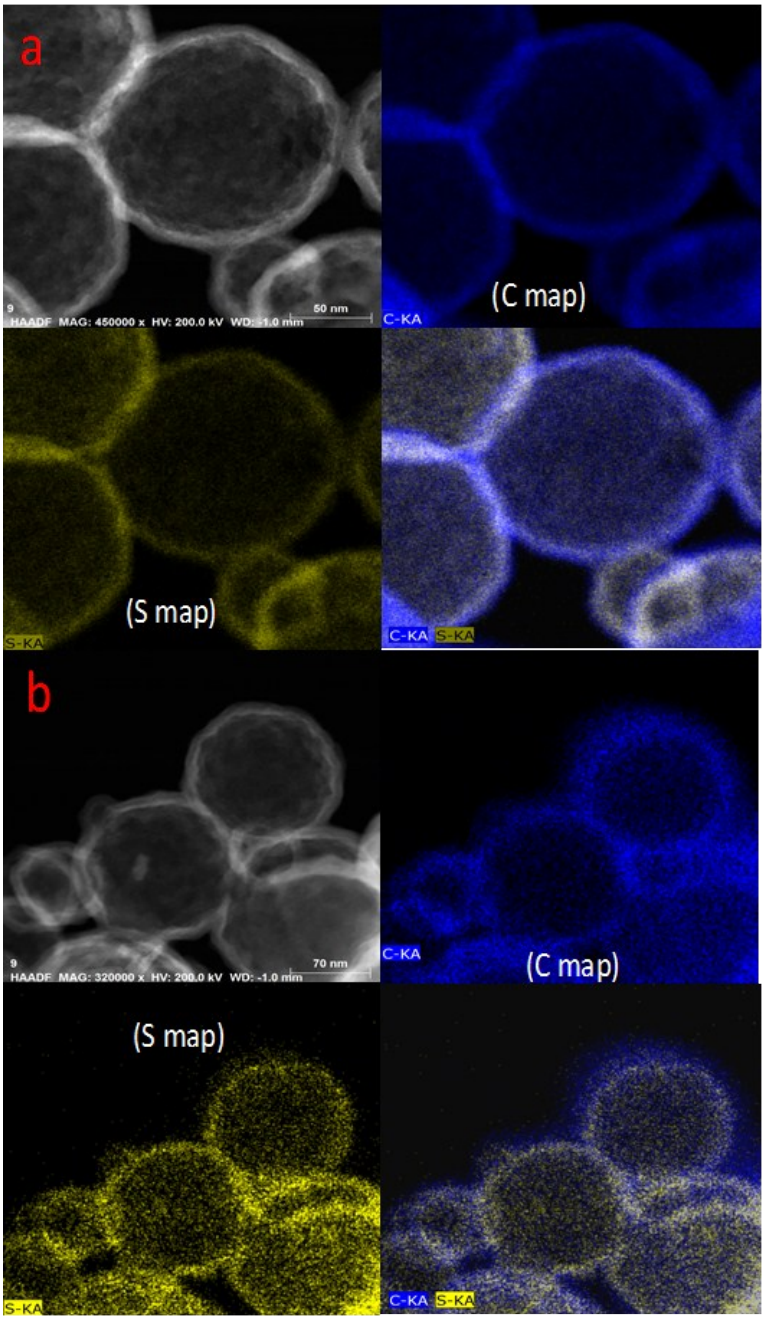

Figure S7. HAADF and EDX element mapping of (a) S@MPC-DHS-1, (b) S@MPC-DHS-3.

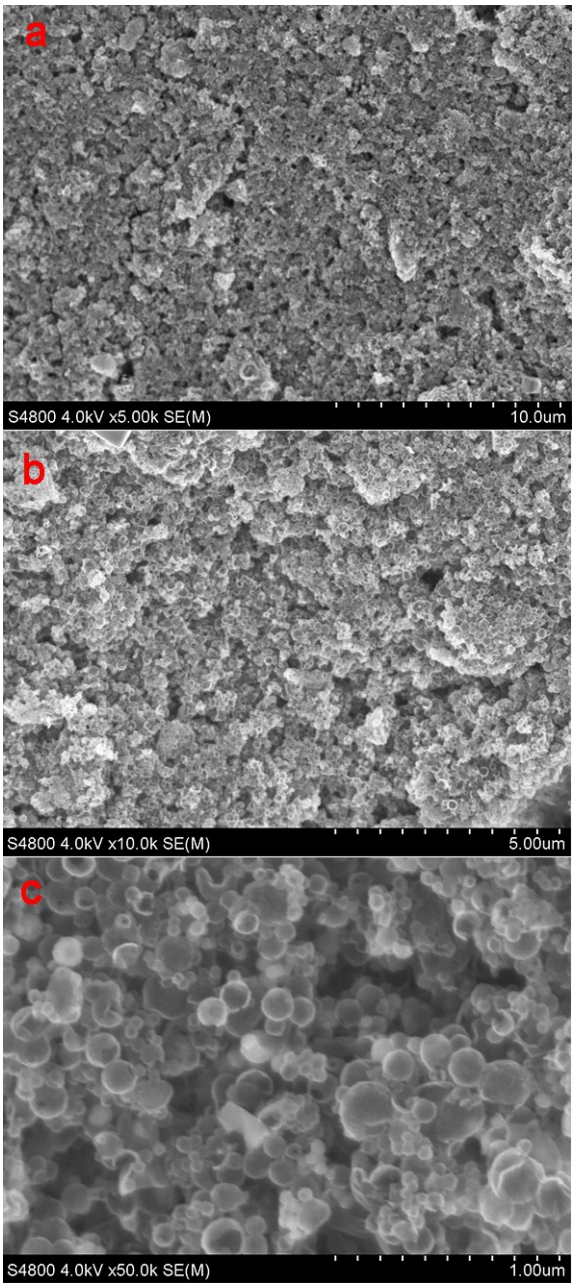

Figure S8. The electrode SEM images of S@MPC-DHS-3 at the magnifications of (a) 5 k, (b) 10 k, and (c) 50 k.

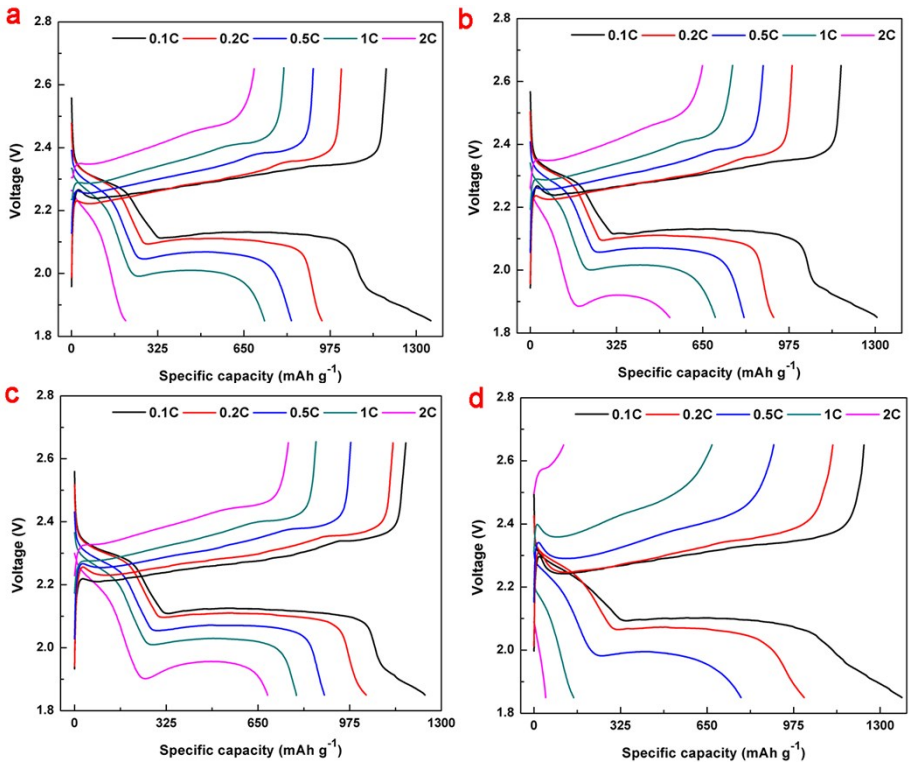

Figure S9. The charge-discharge curves of (a) S@MPC-DHS-1, (b) S@MPC-DHS-2, (c) S@MPC-DHS-3, and (d) S@MPC-DHS-4 at different current rates.

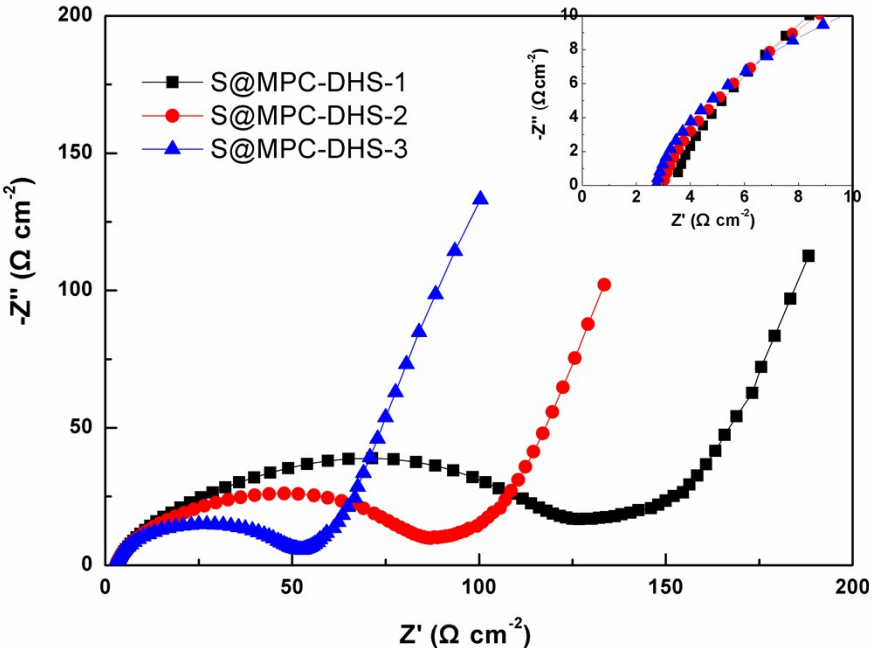

Figure S10. Electrochemical impedance spectroscope (EIS) of S@MPC-DHS-1, S@MPC-DHS-2 and S@MPC-DHS-3.

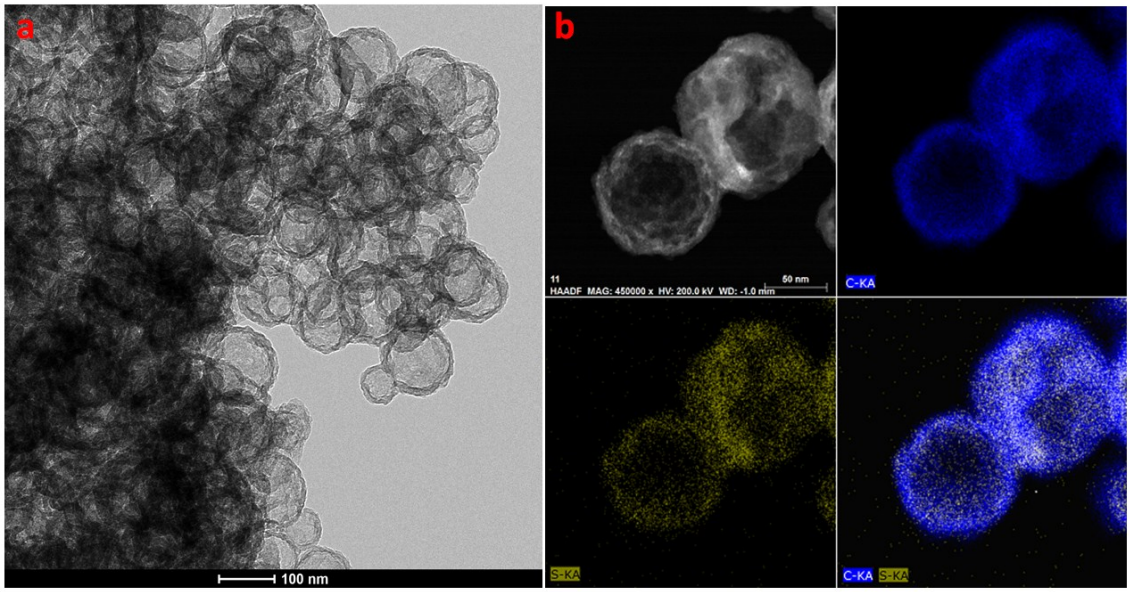

Figure S11. (a) The TEM and (b) HAADF and EDX element mapping of the S@MPC-DHS-3 after 1000 cycles in cells.

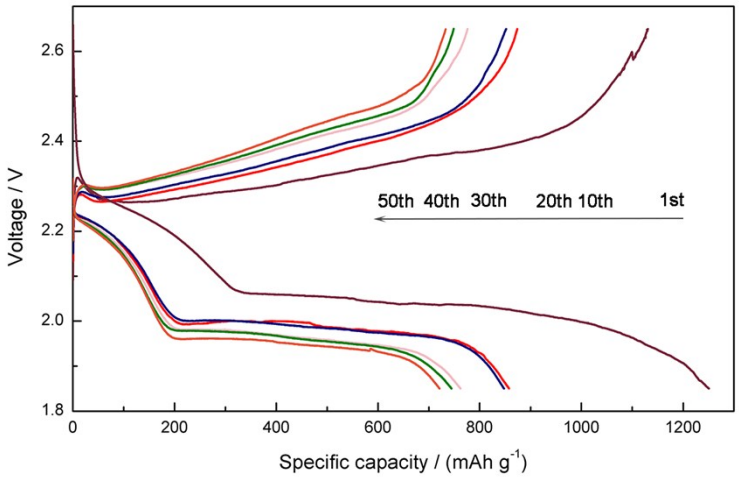

Figure S12. The charge-discharge curves of S@MPC-DHS-3 at 0.05 C-rates under the sulfur loading of 4.4 mg cm^{-2}.

Table S1. The performance parameters comparison of the reported similar materials

Type	Initial discharge capacity (mAh g^{-1})	Reversible discharge capacity (mAh g^{-1})	Current rate (mAh g^{-1})	Number of cycles	S loading (mg cm^{-2})	Sulfur impregnation	Ref.
Porous hollow carbon spheres	1020	690	0.1 C	100	-	400 ℃	[1]
Porous hollow carbon spheres	850	580	0.2 C	500	2.5	140 ℃	[2]
Mesoporous Porous hollow carbon spheres	972	875	1 C	100	1.12-1.4	155 ℃	[3]
Yolk–Shell Structure	919	628	0.5 C	200	2	180 ℃	[4]
Hierarchical Porous Carbon	1163.9	665	0.5 C	200	1	155 ℃	[5]
	1049	512.2	2 C	200			
	753.2	343.8	4 C	200			
Nitrogen-Doped Hollow Carbon	740	630	0.6 C	600	1.5	160 ℃	[6]
Double-Shelled Hollow Carbon Spheres	838.7	520	0.5 C	200	3.9 (vacuum filtration)	155 ℃	[7]
Pomegranate-Like Cluster Structure	1010	707	0.5 C	300	2	155 ℃	[8]
Microporous hollow carbon spheres	800	400	1 C	1000	0.6-0.9	25℃	this work
	1017	750	0.1 C	100	2.3		

REFERENCE

1 G. He, S. Evers, X. Liang, M. Cuisinier, A. Garsuch, L.F. Nazar, ACS Nano, 2013, 7, 10920.
2 C. Zhang, H.B. Wu, C. Yuan, Z. Guo, X.W. Lou, Angew. Chem., Int. Ed., 2012, 51, 9592.
3 G. Zhou, Y. Zhao, A. Manthiram, Adv. Energ. Mater. , 2015, 5, 1402263.
4 W. Zhou, Y. Yu, H. Chen, F.J. DiSalvo, H.D. Abruna, J. Am. Chem. Soc., 2013, 135, 16736.
5 W. Li, Z. Liang, Z. Lu, H. Yao, Z.W. Seh, K. Yan, G. Zheng, Y. Cui, Adv. Energ. Mater. , 2015, 5 , 1500211.
6 F.F. Zhang, G. Huang, X.X. Wang, Y.L. Qin, X.C. Du, D.M. Yin, F. Liang, L.M. Wang, Chem. Eur. J. , 2014, 20, 17523.
7 F. Boettger-Hiller, P. Kempe, G. Cox, A. Panchenko, N. Janssen, A. Petzold, T. Thurn-Albrecht, L. Borchardt, M. Rose, S. Kaskel, C. Georgi, H. Lang, S. Spange, Angew. Chem., Int. Ed., 2013, 52 ,6088.
8 W. Zhou, X. Xiao, M. Cai, L. Yang, Nano Lett, 2014, 14, 5250.